Accretion Phenomena and Related Outflows, IAU Colloquium 163
ASP Conference Series, Vol. 121, 1997
D.T. Wickramasinghe, L. Ferrario, and G.V. Bicknell, eds.

Probing Accretion Disks in AGN with Water Masers

Philip R. Maloney

Center for Astrophysics and Space Astronomy, University of Colorado, Boulder, CO 80309-0389

Abstract. Extremely luminous extragalactic water masers - the so-called "megamasers", with isotropic luminosities of tens to hundreds of solar luminosities - appear to be uniquely associated with active galactic nuclei. The recent survey of Braatz et al. indicates that 20% of Seyfert 2 galaxies have detectable water maser emission. Although originally suggested to arise in shocks, it now seems likely that the masers arise from the irradiation of high-pressure molecular gas by X-rays from the AGN. Quantitative modelling shows that the observed megamaser luminosities can plausibly be produced in this fashion. Both observational limits on the size scales and the high gas pressures required indicate that the water maser emission arises on very small scales, either in a circumnuclear "torus" or the accretion disk itself. In the best-studied case, NCG 4258, the masers are produced in a geometrically thin, warped accretion disk. The maser models can be used to derive quantitative information about the physical conditions in the disk, namely, the mass accretion rate, and therefore the radiative efficiency. I discuss the implications of water maser observations and models for the study of accretion disks and circumnuclear tori in AGN.

1. Introduction

Water maser emission in the $6_{16} \rightarrow 5_{23}$ transition at 22 GHz (1.35 cm) is common in late-type stars and star-formation regions throughout the Galaxy. The most luminous Galactic water maser, in W49, occasionally reaches an isotropic luminosity[1] of 1 $L_\odot$, but typical Galactic water maser luminosities are $L \sim 10^{-3}\, L_\odot$ (Genzel & Downes 1979).

Searches for water masers in other galaxies detected a number of sources resembling W49 in the disks of nearby galaxies (e.g., M33: Churchwell et al. 1977). Shortly thereafter, however, an entirely new kind of water maser source was detected in NGC 4945 (dos Santos & Lepine 1979). With an isotropic luminosity $L \sim 100\, L_\odot$, the water maser in NGC 4945 is roughly five orders of magnitude more luminous than typical Galactic masers, and is located in the galactic nucleus. Subsequent searches for additional water "megamasers" over

[1]Maser luminosities are traditionally given as the isotropic value $4\pi D^2 F$, where D is the source distance and F is the line flux, even though, since maser emission is highly anisotropic, this substantially overestimates the true luminosity.

the next five years uncovered four more such sources (cf. Claussen & Lo 1986, and references therein). In all cases the maser emission is centered on the nucleus; the spectra typically show one or more narrow ($\Delta V \sim$ a few km s^{-1}) features near the systemic velocity, with a velocity spread of perhaps 100 km s^{-1} around $V_{\rm sys}$ in the case of multiple components. Significantly, all five of the megamaser sources were found in galaxies which show evidence for nuclear activity. Furthermore, VLA observations of the masers in NGC 1068 and NGC 4258 by Claussen & Lo (1986) showed that the diameters of the emitting regions were less than 3.5 and 1.3 pc, respectively.

Additional surveys for water megamasers, chiefly in late-type and infrared-luminous galaxies, failed to detect any new sources. However, taking a cue from the fact that all five known megamasers occurred in galaxies with active nuclei, Braatz, Wilson & Henkel (1994, 1996) undertook a systematic survey of AGN for water masers, and have detected ten new sources. An additional water maser, with an isotropic luminosity $L \sim 6100\,L_\odot$ (the so-called "gigamaser" source), was detected in the radio galaxy TXFS2226–184 by Koekemoer et al. 1995, bringing the number of megamasers (those sources with $L \gtrsim 20\,L_\odot$) to 16. *All* of the megamasers are in Seyfert 2 or LINER galaxies; as with the first five, the maser emission is centered on the nucleus. Table 1, adopted from Braatz et al. 1996, lists the luminosities and galaxy type for the megamasers known at this time. (Since many of these sources vary substantially in flux, the quoted luminosities are epoch-dependent: see Braatz et al. for details and references.)

Table 1. **Megamaser Sources**

Galaxy	Type	$L_{\rm H_2O}$ ($L_\odot$)
NGC 4945	Sy 2	57
Circinus	Sy 2	24
NGC 1068	Sy 2	170
NGC 4258	LINER	85
NGC 3079	LINER	520
Mrk 1	Sy 2	64
NGC 1052	LINER/Radio	200
Mrk 1210	Sy 2	99
NGC 2639	LINER	71
NGC 5506	Sy 2	61
TXFS2226–184	LINER/Radio	6100
NGC 1386	Sy 2	120
ESO 103–G35	Sy 2	360
IC 2560	Sy 2	130
IC 1481	LINER	320
NGC 5347	Sy 2	32

The Braatz et al. survey makes it possible to make some quantitative statements about megamaser statistics. One of the most remarkable results is that the fraction of AGN with H_2O megamasers is in fact not small. Of the AGN with recessional velocities $cz < 7000$ km s^{-1}, 5.4% have detectable water maser

https://doi.org/10.1017/S025292110004255X Published online by Cambridge University Press

emission. For $cz < 2000\,\mathrm{km\ s^{-1}}$, the limit to which a maser as luminous as that of NGC 4258 could have been detected for the whole sample, this fraction increases to 11%. For Seyfert 2 galaxies the numbers are even more remarkable: 7% for $cz < 7000\,\mathrm{km\ s^{-1}}$ and 21% for $cz < 2000\,\mathrm{km\ s^{-1}}$. For LINERS these numbers are 7.5% and 9%, while no H_2O megamasers have been detected in Type 1 Seyferts. Thus either several percent of AGN produce detectable water maser emission, or all AGN are in fact megamaser sources and the solid angle of the emission around the nucleus is of order ten percent. The latter interpretation is suggested by the exceptionally large fraction of detected Type 2 Seyferts and the failure to date to find any water megamasers in Type 1 Seyferts: in the unified scheme for AGN (e.g., Antonucci 1993), our line of sight passes through the obscuring material in Type 2 objects, but misses it (we see "down the pipe") in Type 1 objects. Since maser emission is inherently strongly beamed, we will detect Sy 2s and not Sy 1s if the beaming is in the plane of the obscuring material (Braatz et al. 1994), whether this is the accretion disk itself or a geometrically thick "torus" (Krolik & Begelman 1986, 1988).

2. The Origin of H_2O Megamasers

The close association between the presence of an AGN and luminous water maser emission suggests a direct physical connection, a suggestion which is reinforced by the fact that the emission in NGC 1068 and NGC 4258 was found to arise within $r \sim 1$pc or less of the nucleus (Claussen & Lo 1986). Furthermore, in several megamaser sources, the maser emission was found to extend to velocities substantially away from systemic: $V_{\mathrm{maser}} = V_{\mathrm{sys}} \pm 180 - 370\,\mathrm{km\ s^{-1}}$ for NGC 1068, NGC 3079, NGC 4945, and Circinus (Claussen & Lo 1986; Haschick & Baan 1985; Nakai et al. 1995), and most spectacularly, $V_{\mathrm{maser}} = V_{\mathrm{sys}} \pm 1000\,\mathrm{km\ s^{-1}}$ in NGC 4258 (Nakai, Inoue & Miyoshi 1993). Claussen & Lo (1986) suggested that water megamasers might arise in the circumnuclear tori postulated to explain the differences between Type 1 and Type 2 Seyferts, perhaps as a result of the interaction between a nuclear wind and the torus.

Several of the megamaser sources are known to possess luminous X-ray sources ($L_X \gtrsim 10^{42}$ erg s^{-1}) with large attenuating column densities ($N_H \sim 4 \times 10^{22} - 10^{25}$ cm^{-2}), indicating the presence of "buried" AGN. For example, NGC 4945 has a nuclear X-ray source with a luminosity of $L_X \approx 2 \times 10^{42}$ erg s^{-1} buried behind a column of 5×10^{24} cm^{-2}; at 100 keV it is actually the second brightest Seyfert galaxy (Iwasawa et al. 1993; Done, Madejski & Smith 1996).

This close connection between H_2O megamasers and obscured AGN led Neufeld, Maloney & Conger (1994) (hereafter NMC) to investigate whether the maser emission could be a direct consequence of the irradiation of dense circumnuclear gas (the torus) by X-rays from the active nucleus. At high pressures (and the gas pressure must be high near the AGN in consequence of the absorbed radiation pressure), neutral-neutral reactions between molecular hydrogen, atomic oxygen, and OH are very efficient at forming water, provided that X-ray heating keeps the gas temperature $T \gtrsim 300$ K (to overcome the activation energy barriers) but is not so large that molecular hydrogen is not abundant. Much of the gas-phase oxygen can be incorporated into water, which for solar

https://doi.org/10.1017/S025292110004255X Published online by Cambridge University Press

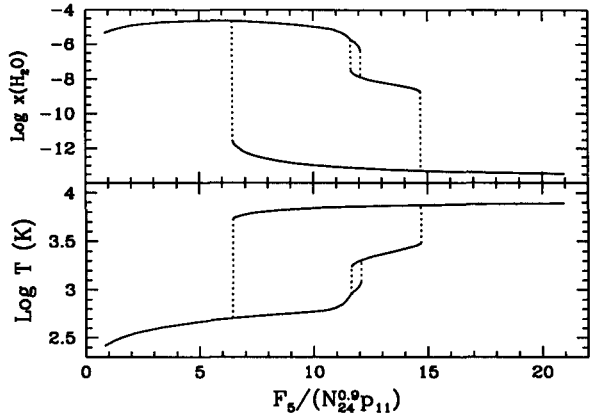

Figure 1. Gas temperature and water abundance as a function of X-ray flux $F_X = 10^5 F_5$ erg s^{-1}, pressure $P/k = 10^{11} P_{11}$ cm^{-3} K, and shielding column $10^{24} N_{24}$ cm^{-2}.

abundances means that the water abundance relative to the density of hydrogen nuclei $x(H_2O) = n(H_2O)/n(H)$ can approach 10^{-4}.

Figure 1 shows the water abundance and gas temperature obtained by NMC, as a function of the X-ray flux, for an isobaric semi-infinite slab (the inner edge of a geometrically thick torus). Two phases are possible for the torus: a warm ($T \sim 8000$ K), weakly ionized (electron fraction $x_e \sim 0.01 - 0.1$) atomic phase and a cooler ($T \sim 600 - 1000$ K) molecular phase with negligible ionization ($x_e \lesssim 10^{-5}$). (The intermediate phase at $T \sim 2000$ K is generally not present.) Note the scaling parameter on the abscissa is not the incident X-ray flux, but an effective ionization parameter: the X-ray flux divided by the gas pressure and the attenuating column density (the column between the X-ray source and the point of interest) to the 0.9 power. (The precise value of the column density exponent depends weakly on the spectral index; see Maloney, Hollenbach & Tielens 1996.) Thus the conditions in the gas will vary not only with the incident X-ray flux and pressure, but also with column density into the torus; this is simply the consequence of the attenuation of the X-ray flux, and therefore a decrease in the ionization and heating rates, with increasing column into the torus. Although both the atomic and molecular phase can coexist over a range in the ionization parameter, there is a maximum value above which the gas must be in the atomic phase, and similarly a minimum value below which the gas must be molecular. As we will see shortly, the presence of this phase transition between warm atomic and molecular gas has important implications.

The structure of an irradiated torus is shown explicitly in Figure 2, which is plotted as a function of depth rather than ionization parameter. The surface of the torus is kept atomic and warm by the incident X-ray flux. As the ionization and heating rates drop with increasing depth, the torus eventually undergoes a transition to the molecular phase, and the water abundance jumps from negligible values to $x(H_2O) \sim 10^{-4}$.

https://doi.org/10.1017/S025292110004255X Published online by Cambridge University Press

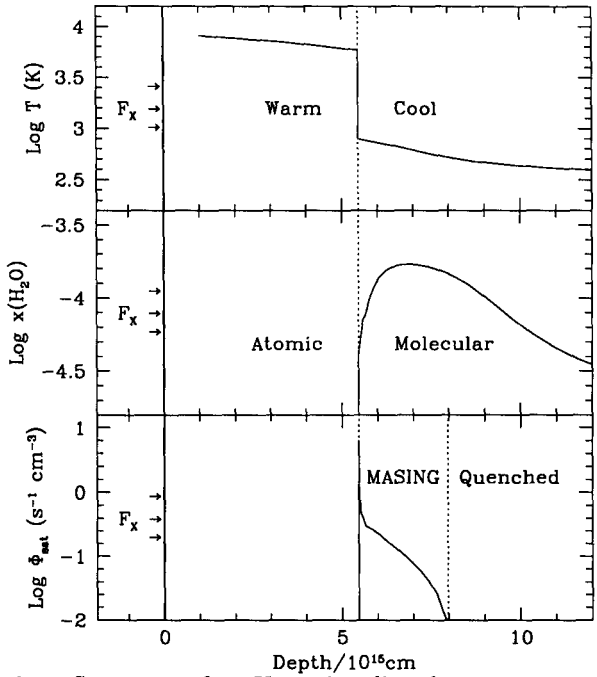

Figure 2. Structure of an X-ray irradiated torus; see text

In the molecular zone, the temperature is initially close to 1000 K, so the H_2 density is approximately 10^8 cm^{-3}. (The torus pressure in this model has been fixed at $\tilde{P} = P/k = 10^{11}$ cm^{-3} K.) The rotational levels which produce the 22 GHz maser line lie about 600 K above the ground state, so the gas temperature must be a few hundred K in order to excite them. The magnitudes of the relevant radiative transition rates are such that inversion of the level populations – which can be produced simply by collisions in H_2O (Elitzur 1992) – requires H_2 densities between 10^7 and 10^{10} cm^{-3}; if the densities are too low there is negligible population in the 6_{16} and 5_{23} levels, while if they are too high collisions thermalize the levels and quench the masing. Thus conditions in the molecular zone are ideal for collisionally pumping 22 GHz maser emission, provided that the torus gas pressure $10^{10} \lesssim \tilde{P} \lesssim 10^{13}$. As indicated in Figure 2, masing is eventually quenched by radiative trapping in the far-infrared transitions connecting the rotational levels, which leads to thermalization of the masing levels (de Jong 1973). Over a wide range of pressures and X-ray fluxes, the resulting maser luminosities are $L_{H_2O} \sim 10^{2\pm0.5}$ per pc^2 of illuminated area, which, for $r \sim$ pc-scale tori, is large enough to explain most of the observed isotropic luminosities (NMC). As pointed out by Collison & Watson (1995), absorption of the far-infrared non-masing photons by dust grains can inhibit quenching of the maser action as long as the gas is substantially hotter than the dust, although the importance of this process depends on the gas pressure (it is important at

https://doi.org/10.1017/S025292110004255X Published online by Cambridge University Press

$\tilde{P} \sim 10^{11}$ cm^{-3} K and negligible at $\tilde{P} \sim 10^{12}$ cm^{-3} K) and the geometry. This could in some cases raise the maser luminosities above those calculated by NMC.

Powering of the water maser emission via irradiation of the inner edge of a geometrically thick torus by X-rays from the central source therefore offered an attractive model for H_2O megamasers, which could be directly tested by VLBI observations. However, the first megamaser source to be studied in detail with VLBI indicated that this model, if not stood on its head, at least had to be turned on its side.

3. The Warped Maser Disk of NGC 4258

The water maser emission in NGC 4258 was already distinguished even in single-dish observations by having the largest velocity spread away from systemic, as noted earlier, with $V_{\rm maser} = V_{\rm sys} \pm 1000$ km s^{-1}. VLBI observations of the maser features (Miyoshi et al. 1995; Greenhill et al. 1995a) revealed two more remarkable features: (1) The maser emission arises in a thin, warped disk, with an inner radius of 0.13 pc and an outer radius of 0.25 pc; the vertical thickness to radius ratio $H/R < 0.0025$ at the location of the systemic features. (2) The rotation curve defined by the maser features is perfectly Keplerian to within the measurement errors. The mass enclosed within 0.13 pc is $M_c = 3.6 \times 10^7 M_\odot$, giving a lower limit to the central mass density of $\rho_c > 4 \times 10^9 M_\odot$ pc^{-3}. This large central density and the Keplerian rotation curve essentially rule out alternatives to a massive black hole (e.g., Maoz 1995). Furthermore, since the central active nucleus has been directly detected in X-rays (Makashima et al. 1994), it is possible to determine the fractional Eddington luminosity, which is surprisingly small: $L/L_E \sim 10^{-4}$ (Neufeld & Maloney 1995). A nice summary of the observations and implications is given by Moran et al. (1995). Contrary to assertions elsewhere in the literature, Miyoshi et al. (1995) did *not* derive a density in the disk of $n_{\rm H_2} = 10^{10}$ cm^{-3}; they merely pointed out that this was the maximum possible density the disk could have without quenching the maser emission, as noted above.

The inferred geometry of the water maser emission is shown in Figure 3, which shows the best-fitting warped disk model from Herrnstein et al. (1995). The systemic velocity features lie along the central line of sight, while the high-velocity features lie along the midline of the disk perpendicular to our line of sight. Independent confirmation that this is the correct geometry is provided by observations of centripetal accelerations of the maser features; the systemic features have a measured acceleration of $a \sim 9$ km s^{-1} yr^{-1}, while the high-velocity features have accelerations $a < 1$ km s^{-1} yr^{-1} (Greenhill et al. 1995b). The best determination is for the bright high-velocity feature at 1306 km s^{-1} (Herrnstein et al. 1996) which gives $a = 0.0 \pm 0.1$ km s^{-1} yr^{-1}, constraining this feature to lie within about two degrees of the perpendicular midline. Measurement of the centripetal acceleration of the systemic-velocity features also makes it possible to obtain a direct geometric distance to NGC 4258 (Miyoshi et al. 1995).

Clearly the water maser emission in NGC 4258 is not arising from the irradiated inner surface of a geometrically thick torus. However, the fact that the disk is *observed* to be warped suggests that the maser disk is being obliquely illuminated by the central X-ray source, and that this is what powers the maser emis-

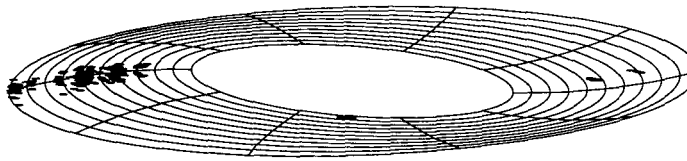

Figure 3. The geometry of the warped maser disk in NGC 4258.

sion. To quantitatively investigate this possibility, Neufeld & Maloney (1995) (hereafter NM) modeled the disk using the standard $\alpha-$prescription for viscosity: $\nu = \alpha c_s H$, where c_s is the gas sound speed and H is the disk vertical scale height, and $0 < \alpha \leq 1$. Since radiative heating due to irradiation by the central X-ray source dominates over viscous heating, this is not a standard Shakura-Sunyaev $\alpha-$disk. Ignoring self-gravity, the disk scale height is

$$H = \frac{c_s}{V_{\rm orb}} R = 2.6 \times 10^{14} \frac{T_3^{1/2} R_{0.1}^{3/2}}{M_8^{1/2}} \ {\rm cm} \tag{1}$$

where the gas temperature $T = 1000 T_3$ K, the radius is $R = 0.1 R_{0.1}$ pc, and the central mass is $M_c = 10^8 M_8 \, M_\odot$. Since the gas temperature $T_3 \sim 1 - 10$ in the radius range of interest, the disk will be extremely thin. The disk midplane pressure is large:

$$\tilde{P} = 1.3 \times 10^{11} \frac{M_8 \dot{M}_{-5}}{\alpha R_{0.1}^3} \ {\rm cm}^{-3} \ {\rm K} \tag{2}$$

where the mass accretion rate through the disk is $\dot{M} = 10^{-5} \dot{M}_{-5} \, M_\odot \ {\rm yr}^{-1}$, and $c_s = 7 \ {\rm km \ s}^{-1}$ ($T \approx 8000$ K) has been assumed. Note that the gas pressure in the disk decreases as R^{-3}.

If the maser action is due to X-ray heating of the irradiated warped disk surface, why does masing occur over only a limited range of radii? To answer this question, return to Figure 1 for a moment. The *minimum* value of the ionization parameter at which the gas can remain atomic (the left endpoint of the upper solid line in the lower half of Figure 1) corresponds to a *maximum* pressure at which the gas can remain atomic; for pressures higher than this critical value, the gas must be molecular. This critical pressure can be written as

$$\tilde{P}_{\rm cr} \approx 3.3 \times 10^{10} \frac{L_{41}}{R_{0.1}^2 N_{24}^{0.9}} \ {\rm cm}^{-3} \ {\rm K} \tag{3}$$

where the 2−10 keV X-ray luminosity $L_X = 10^{41} L_{41}$ erg s^{-1} and $10^{24} N_{24}$ cm^{-2} is the shielding column density of hydrogen nuclei. Because the flux drops as R^{-2}, this critical pressure decreases less rapidly with radius than the disk pressure (i.e., the ionization parameter *increases* with radius), and so the critical radius for molecule formation is given by

$$R_{cr} = 0.04 \frac{(\dot{M}_{-5}/\alpha)^{0.81} M_8^{0.62}}{L_{41}^{0.43} \mu^{0.38}} \ {\rm pc} \tag{4}$$

https://doi.org/10.1017/S025292110004255X Published online by Cambridge University Press

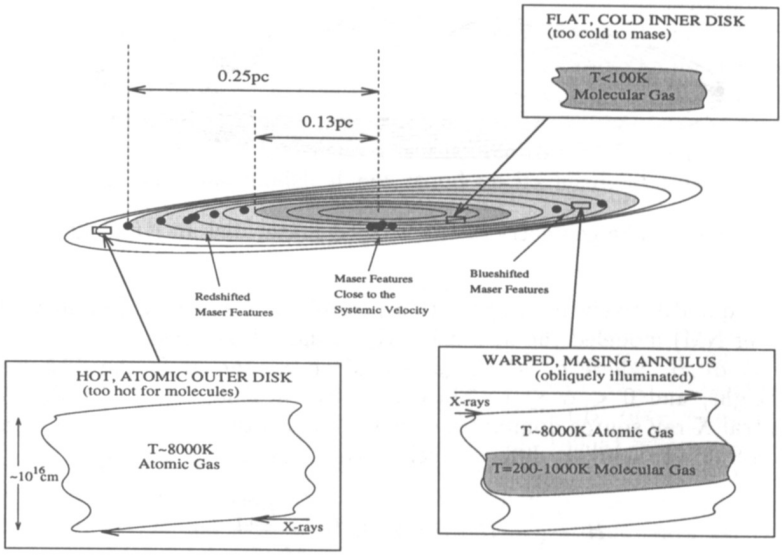

Figure 4. Thermal/maser structure of the NGC 4258 disk.

including a correction for the fact that the disk is obliquely illuminated at an angle $\cos^{-1}\mu$. At radii $R < R_{cr}$, the disk will be molecular at a temperature of a few hundred K, while for radii $R > R_{cr}$ the gas will be warm ($T \sim 8000$ K) and atomic. Thus the *outer* radius of the masing disk, at $R = 0.25$ pc, should be identified with the phase transition from atomic to molecular gas; as in NMC, the conditions in the molecular gas in this region will be ideal for producing 22 GHz maser emission. The inferred structure of the disk is shown in Figure 4. For NGC 4258, $L_{41} = 0.4$ (Makashima et al. 1994), $M_8 = 0.36$, and $\mu \approx 0.25$ at the outer edge of the masing zone, so with $R_{cr} = 0.25$ pc, we find

$$\frac{\dot{M}}{\alpha} \approx 7 \times 10^{-5}\ M_\odot\ \mathrm{yr}^{-1} \tag{5}$$

for the mass accretion rate through the disk. If $\dot{M}$ has stayed constant over the timescale it takes gas to be viscously transported from 0.25 pc to the central black hole ($\tau_{\rm acc} \sim 4 \times 10^6$ years), then the efficiency of conversion of rest-mass energy into X-rays is $\alpha\epsilon_X \sim 0.01$. Since $2-10$ keV X-rays typically account for 10% of the bolometric luminosity of an AGN (Mushotsky, Done & Pounds 1993), the total efficiency for energy generation is $\epsilon \sim 0.1/\alpha$, in remarkable agreement with theoretical expectations for $\alpha \sim 1$. This result indicates that the low luminosity of the AGN in NGC 4258 is a consequence of a low mass accretion rate, not the extremely low-efficiency ($\epsilon \sim 10^{-3}$) of an advection-dominated accretion disk (Lasota et al. 1996). As also noted by NM, the scalings of maser luminosity with M_c and L suggest the possibility of water masers far more powerful than any yet known.

This has left unexplained why the inner edge of the masing zone occurs at $R = 0.13$ pc. NM suggested that this marked the location where the warp

https://doi.org/10.1017/S025292110004255X Published online by Cambridge University Press

flattened out; in the absence of irradiation by the central X-ray source, the disk would be too cold to produce abundant water or to excite maser emission. While flattening of the warp at this radius was consistent with the kinematic models of Miyoshi et al. (1995), it begged the question of why the warp flattens out there or, indeed, why the disk is warped at all. Since the potential is essentially Keplerian, an arbitrary imposed warp would be kinematically stable, but this simply moves the question of the origin of the warp back one step.

An explanation for both the origin of the warp and the flattening of the inner disk is provided by the radiation-driven warping instability discovered by Pringle (1996) and explored in greater detail by Maloney, Begelman & Pringle (1996) (MBP). As shown by MPB (see also Maloney & Begelman, this volume) the warp instability both explains the origin of the warp and predicts that only the outer part of the disk will be warped in this case, in agreement with the observations of NGC 4258, provided that the radiative efficiency $\epsilon \sim 0.1$, in agreement with the efficiency and mass accretion rate derived by NM.

An additional puzzle also has a solution in this context. The high-velocity features in NGC 4258 are markedly asymmetric in intensity: the red-shifted features are much stronger than the blue-shifted ones. Herrnstein, Greenhill & Moran (1996) have shown that this asymmetry can be understood quantitatively as the result of free-free absorption in the warm atomic and fully ionized surface zones of the disk; because of the orientation of the disk to our line of sight, only the blue-shifted emission is subject to absorption. Thus we have a completely self-consistent model for the masing and the warping of the disk in NGC 4258.

4. The Masing Torus of NGC 1068

Very recent VLBI observations of NGC 1068 (Greenhill et al. 1996) suggest that, for this galaxy, the geometry originally considered by NMC may be the relevant one. The observations (which so far cover only the systemic and red-shifted maser emission) show that the masers are distributed linearly at a position angle of about $-45°$ which Greenhill et al. interpret as being the inner edge of a geometrically thick ($H/R \sim 1$) torus, with an inner radius $R \sim 0.4$ pc (Figure 5). The axis of the inferred "cone" of maser emission (including the anticipated position of the blue-shifted emission, based on the VLA observations of Gallimore et al. 1996) is identical to the axis of the radio jet. The rotation velocity is sub-Keplerian ($V \propto R^{-0.35}$, and the measured velocity dispersions are both a substantial fraction of the observed orbital velocities and increase rapidly toward the central source. The derived mass within 0.65 pc is $M \sim 10^7 M_\odot$, which makes the fractional Eddington luminosity $L/L_E \sim 0.5$.

Why does NGC 1068 look so different from NGC 4258? The fact that the observed velocities are sub-Keplerian could be the result of either (1) the background stellar cluster: if this is described by a characteristic velocity dispersion σ, the masing zone will only lie in the Keplerian regime if

$$L/L_E \ll 0.77 \left(\frac{\alpha\epsilon}{0.1}\right)^{2.1} \mu \left(\frac{\sigma}{200 \text{ km s}^{-1}}\right)^{-5.3} ; \qquad (6)$$

or (2) large gas velocity dispersions, which will contribute to the support against gravity; in this case the maximum observed velocity difference between the maser

https://doi.org/10.1017/S025292110004255X Published online by Cambridge University Press

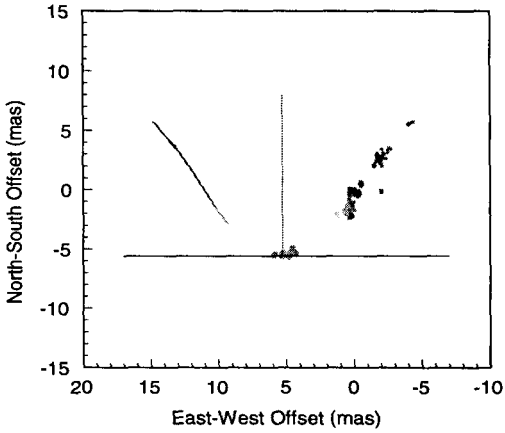

Figure 5. The systemic and redshifted maser emission of NGC 1068. The vertical dotted line is the radio jet axis and the thin line to the left of the jet axis is the expected position of the blue-shifted emission.

and systemic velocities will be the mean streaming velocity rather than the circular velocity. The large observed velocity dispersions suggest that (2) must be important. These same velocity dispersions presumably account for the thickness of the maser distribution. This may be a reflection of the much greater importance of radiation pressure in NGC 1068, which has a much larger fractional Eddington luminosity than NGC 4258. The action of radiation pressure on the gas of the torus may be responsible for maintaining the large velocity dispersions (Pier & Krolik 1992). If this is the case, then one would expect to find thin, Keplerian maser disks only in sources with small fractional Eddington luminosities.

5. Conclusions

At the moment, the close connection between AGN and water megamasers seems to be plausibly understood, as a consequence of the irradiation of dense gas in the nucleus (either a torus or the accretion disk itself) by X-rays from the central source. Alternative models for the maser emission, such as shocks or winds, have also been suggested (e.g., Kartje, Königl, & Elitzur, this conference) but have yet to be worked out in detail. Forthcoming VLBI observations to further test all these scenarios are eagerly awaited. There are already some interesting puzzles. For example, the two megamaser sources in elliptical galaxies (NGC 1052 and TXFS2226-184) have line profiles which are completely different from all the other sources: rather than very narrow components distributed over some velocity range, these two sources exhibit fairly broad ($\Delta V \approx 85\,\mathrm{km\ s^{-1}}$) Gaussian line profiles. The spikiness of the profiles in the other megamaser sources probably indicates that the gain is very high, so the two ellipticals may be simply exhibiting lower-gain maser emission – perhaps because they possess

https://doi.org/10.1017/S025292110004255X Published online by Cambridge University Press

larger-scale, more powerful radio sources to serve as background sources for amplification. Whichever model for the origin of the megamasers proves to be correct, it is clear that H_2O megamasers offer extraordinary probes of accretion disks and tori in AGN.

Acknowledgments. I am grateful to Jim Braatz, Lincoln Greenhill and Jim Herrnstein for data in advance of publication, discussions, and figures (Lincoln and Jim provided figures 5 and 3, respectively). I am also grateful for support from from NASA Long-Term Astrophysics Program grant NAGW-4454, and to Geoff Bicknell for inviting me to Port Douglas.

References

Antonucci, R. 1993, ARAA, 31 473.

Braatz, J.A., Wilson, A.S., & Henkel, C. 1994, ApJ, 437, L99.

Braatz, J.A., Wilson, A.S., & Henkel, C. 1996, ApJS, 106, 51

Churchwell, E., Witzel, A., Huchtmeier, W., Pauliny-Toth, I., Roland, J., & Suben, W. 1977, A&A 54, 969.

Claussen, M. J., & Lo, K.-Y. 1986, ApJ, 308, 592.

Collison, A.J., & Watson, W.D. 1995, ApJ 452, L103.

de Jong, T. 1973, A&A 26, 297.

Done, C., Madejski, G.M., & Smith, D.A. 1996, ApJ 463, L63.

dos Santos, P.M., & Lepine, J.R.D. 1979, Nature, 278, 34.

Elitzur, M. 1992, Astronomical Masers (Dordrecht: Kluwer)

Gallimore, J.E., Baum, S.A., O'Dea, C.P., Brinks, E., & Pedlar, A. 1996, ApJ 462, 740.

Genzel, R., & Downes, D. 1979, A&A 72, 234.

Greenhill, L.J., Gwinn, C.R., Antonucci, R., & Barvainis, R. 1996, ApJ (Letters), in press.

Greenhill, L.J., Jiang, D.R., Moran, J.M., Reid, M.J., Lo, K.Y., & Claussen, M.J. 1995a, ApJ, 440, 619.

Greenhill, L.J., Henkel, C., Becker, R., Wilson, T.L., & Wouterloot, J.G.A. 1995b, A&A, 304, 21.

Haschick, A.D., & Baan, W.A. 1985, Nature, 314, 144.

Herrnstein, J., Greenhill, L., & Moran, J. 1996, ApJ, 468, L17.

Herrnstein, J., Moran. J., Greenhill, L., Diamond, P., Miyoshi, M., Nakai, N., & Inoue, M. 1996, in The Physics of Liners in View of Recent Observations, ed. M. Eracleous, A.P. Koratkar, L.C. Ho, & C. Leitherer (San Francisco: Astr. Soc. of the Pacific), in press.

Iwasawa, K., Koyama, K., Awaki, H., Kunieda, H., Makishima, K., Tsuru, T., Ohashi, T., & Nakai, N. 1993, ApJ 409, 155.

Koekemoer, A.M., Henkel, C., Greenhill, L.J., Dey, A., van Breugel, W., Codella, C., & Antonucci, R. 1995, Nature, 378, 697.

Krolik, J.H., & Begelman, M.C. 1986, ApJ, 308, L55.

Krolik, J.H., & Begelman, M.C. 1988, ApJ, 329, 702.

Lasota, J.P., Abramowicz, M.A., Chen, X., Krolik, J., Narayan, R., & Yi, I. 1996, ApJ, 462, 162.

Makishima, K., Fujimoto, R., Ishisaki, Y., Kii, T., Loewenstein, M., Mushotzky, R., Serlemitsos, P., Sonobe, T., Tashiro, M., & Yaqoob, T. 1994, PASJ, 46, L77.

Maloney, P.R., Begelman, M.C., & Pringle, J.E. 1996, ApJ, in press.

Maloney, P.R., Hollenbach, D.J., & Tielens, A.G.G.M. 1996, ApJ 466, 561.

Maoz, E. 1995, ApJ, 447, L91.

Miyoshi, M., Moran, J., Herrnstein, J., Greenhill, L., Nakai, N., Diamond, P., & Inoue, M. 1995, Nature, 373, 127.

Moran. J., Greenhill, L., Herrnstein, J., Diamond, P., Miyoshi, M., Nakai, N., & Inoue, M. 1996, in Quasars and AGN: High Resolution Imaging, Proc. Nat. Acad. Sci., in press.

Mushotsky, R., Done, C., & Pounds, K. A. 1993, ARAA 31, 717.

Nakai, N., Inoue, M., & Miyoshi, M. 1993, Nature, 361, 45.

Nakai, N., Inoue, M., Miyazawa, K., & Hall, P. 1995, PASJ 47, 771.

Neufeld, D.A., & Maloney, P.R. 1995, ApJ, 447, L19.

Neufeld, D.A., Maloney, P.R., & Conger, S. 1994, ApJ, 436, L127.

Pier, E.A., & Krolik, J.H. 1992, ApJ, 399, L23

Pringle, J.E. 1996, MNRAS, 281, 357.

Shakura, N.I., & Sunyaev, R.A. 1973 A&A 24, 337.

Discussion

M. Begelman: Suppose that all of these megamasers arose from their disks. How close to edge-on would these disks have to be in order to see the masers?

P. Maloney: The solid angle of the disk is dominated entirely by the pressure of the warp; if the amplitude of the warp in NGC 4258 is typical, then the masing will be visible within $\sim \pm 10°$ of edge-on.

C. Heisler: There are several Seyfert 2 galaxies in your list that have broad line regions as detected by polarised spectroscopy – do you see any correlations with maser activity and whether or not there is a "hidden" broad line region?

P. Maloney: That is an interesting question which I don't offhand know the answer to; the most systematic work on megamasers has been done by James Braatz (U. Maryland), but not all his work has been published yet.

A. Konigl: Spectropolarmetric observations of NGC 4258 by Wilkes et al. (1995) have indicated that the bolometric luminosity of this source might be higher then what the modified α-disk model could account for. An alternative model, which does not suffer from this potential difficulty and which also accounts naturally for the observation of NGC 1068 has been proposed by Koitze, Konigl & Elitzen (poster in this meeting) and interprets the masers as dense clouds embedded in a hydromagnetic disk wind beyond the dust sublimination radius (where the dust provides most of the requisite shielding from the central continuum radiation).

P. Maloney: The most likely scatterer in NGC 4258 is dust, in which case the inferred bolometric luminosity $L_{BOL} \sim 10^{42}$ erg s^{-1}, only a factor of ~ 2 higher than inferred earlier. (See Gary Schmidt's comment).

Since the masers in NGC 4258 occur where the central source illuminates the warped disk, in my opinion (admittedly biased) this argues for the X-Ray irradiation model. There is also a natural explanation for the differences between NGC 4258 and NGC 1068 in this scenario: For small L/L_E (as in NGC 4258) radiation pressure is negligible compared to gravity, leading to a thin Keplerian disk; at high L/L_E radiation pressure may produce a thick disk (a "torus") with high velocity dispersion (and therefore a non-Keplerian rotation curve).

E. Maoz: The thickness of the masing zone and the quenched zone depend on the abundance of IR photons which tend to thermalise the energy levels. Therefore, the structure of the disk is sensitive to the dust abundance, which is likely to be relatively high, and to velocity gradients over the masing slab, which are clearly present in a rotating disk. Did you take these factors into account in your derivation of the disk structure in NGC 4258?

P. Maloney: Dust can increase the thickness of the masing zone – and therefore the maser luminosity per square parsec of irradiated gas – by absorbing the mid- and far-IR photons which would otherwise thermalise the masing levels. The importance of this process depends on pressure (it is negligible at high gas pressures, $P/K \geq 10^{11}$ cm^{-3} K) and geometry, even if it is important. However, it has NO effect on the disk structure: the pressure at which the disk goes from atomic to molecular – which is where masing begins – is completely independent of whether the maser luminosity is enhanced by dust trapping of photons. Even saturated masing lines provide a negligible fraction of the total cooling.

Velocity fields in the rotating disk likewise determine where maser amplification will be large (and as already noted, the masers in NGC 4258 occur exactly where one would expect the amplification to be large) but have no effect on the location of the atomic-to-molecular phase transition.

G. Schmidt: A comment regarding A. Konigl's question about the luminosity of the NGC 4258 central engine: The luminosity inferred from the reflected spectrum (Wilkes et al. 1995, ApJ, 455, L13) is highly model-dependent. In particular, it depends on the nature of the scattering particles. For dust grains, the most likely agent in this object, the implied luminosity of the central engine is low, $\sim 10^{42}$ erg s^{-1}.